Assessment of the healing process after percutaneous implantation of a cardiovascular device: a systematic review

Elodie Perdreau, Zakaria Jalal, Richard Walton, Jérôme Naulin, Julie Magat, B. Quesson, Hubert Cochet, Olivier Bernus, Jean-Benoît Thambo

Query Details Back to Main Page

1. Kindly check and confirm whether the corresponding author's affiliations were correctly identified and amend if necessary.

The affiliation number 1 is the same as number 6 so you can remove the affiliation number 6 for the corresponding author.
Only 5 affiliations (number 1 to number 5) are therefore confirmed.

2. Kindly check and confirm all level section headings.

the section headings were checked and confirm.

3. Kindly check and confirm the sections under 'Compliance with Ethical Standards' heading.

The sections were checked and confirmed.

Assessment of the healing process after percutaneous implantation of a cardiovascular device: a systematic review

Elodie Perdreau, [1,2,3,6]✉

Email elodie.perdreau@chu-lyon.fr

Zakaria Jalal, [1,2,3,4]

Richard D. Walton, [1,2,3]

Jérôme Naulin, [1,2,3]

Julie Magat, [1,2,3]

Bruno Quesson, [1,2,3]

Hubert Cochet, [1,2,3,5]

Olivier Bernus, [1,2,3]

Jean-Benoît Thambo, [1,2,3,4]

[1] IHU Liryc, Electrophysiology and Heart Modeling Institute, Fondation Bordeaux Université, 33600 Pessac- Bordeaux, France

[2] Université de Bordeaux, Centre de recherche Cardio-Thoracique de Bordeaux, U1045, 33000 Bordeaux, France

[3] INSERM, Centre de recherche Cardio-Thoracique de Bordeaux, U1045, 33000 Bordeaux, France

[4] Congenital and Pediatric Cardiology Unit, Bordeaux University Hospital (CHU), 33600 Pessac, France

[5] Bordeaux University Hospital (CHU), Cardiothoracic Pole, 33600 Pessac, France

[6] IHU Liryc, Avenue du Haut-Lévêque, 33600 Pessac cedex, France this affiliation is the same as number 1

Received: 19 August 2019 / Accepted: 10 November 2019

Abstract

The healing process, occurring after intra-cardiac and intra-vascular device implantation, starts with fibrin condensation and attraction of inflammatory cells, followed by the formation of fibrous tissue that slowly covers the device. The duration of this process is variable and may be incomplete, which can lead to thrombus formation, dislodgement of the device or stenosis. To better understand this process and the neotissue formation, animal models were developed: small (rats and rabbits) and large (sheep, pigs, dogs and baboons) animal models for intra-vascular device implantation; sheep and pigs for intra-cardiac device implantation. After intra-vascular and intra-cardiac device implantation in these animal models, in vitro techniques, i.e. histology, which is the gold standard and scanning electron microscopy, were used to assess the

device coverage, characterize the cell constitution and detect complications such as thrombosis. In humans, optical coherence tomography and intra-vascular ultrasounds are both invasive modalities used after stent implantation to assess the structure of the vessels, atheroma plaque and complications. Non-invasive techniques (computed tomography and magnetic resonance imaging) are in development in humans and animal models for tissue characterization (fibrosis), device remodeling evaluation and device implantation complications (thrombosis and stenosis). This review aims to (1) present the experimental models used to study this process on cardiac devices; (2) focus on the in vitro techniques and invasive modalities used currently in humans for intra-vascular and intra-cardiac devices and (3) assess the future developments of non-invasive techniques in animal models and humans for intra-cardiac devices.

AQ1

Keywords

Healing process
Cardiac device
Histology
Thrombosis
Imaging techniques
Animal models

Introduction

The healing process is an important stage that follows intra-cardiac and intra-vascular device implantation and leads to the formation of a neotissue covering the device [1]. It usually starts with fibrin condensation and an intense inflammatory reaction, involving cells that migrate from neighboring regions (host fibroblast-like cells, macrophages, lymphocytes, endothelial mature cells), extra-cellular matrix and thrombotic material. Circulating endothelial progenitors are also attracted, as well as angiogenic growth factors. It is followed by the formation of a poorly vascularized granulating tissue, slowly covering the device and evolving towards fibrosis, predominantly made of collagen and small vessels [2, 3, 4]. Chronic inflammatory reactions with multinucleated cells and lymphocyte infiltration may also be observed [4].

Ideally, device coverage should occur over a short time-course, be uniform and complete after implantation [1, 5]. The duration of this process is highly variable across different studies, depending on the environment (in vivo or in vitro) and device, its location in the heart and its material composition [2, 6]. In animal models, the healing process occurs between 28 and 90 days [7, 8]; in humans, between 6 and 18 months [9]. However, this process may be much longer, as some devices still remain uncovered 2 years after implantation, such as first-generation sirolimus-eluting stents [10], atrio-septal device defect occlusion devices or left atrial appendage occluders [11, 12].

The thickness of the neotissue that develops on the inner surface of stents presents a great variability, from a few microns to a few millimiters, depending on multiple factors such as the type of device, implantation time, age of human or animal [3, 13, 14].

With the recent development of numerous percutaneous devices, this process is more studied. Intra-vascular devices such as stents and vascular prosthesis, and intra-cardiac devices, such as atrio/ventricular septal defect occluders and left atrial appendage occluders, are concerned by this natural process and its potential short- and long-term complications. Indeed, in case of an incomplete or late device tissue coverage, thrombus formation, endocarditis, stent stenosis or dislodgement of the device can complicate the issue after implantation [11, 12, 15, 16]. Thereby, strut coverage of a coronary stent was demonstrated to be a powerful histological predictor of stent thrombosis [17, 18]. Several factors were suspected to lead to late stent stenosis : the anti-proliferative drug of the device that not only prevented smooth muscle cell proliferation but also endothelialization; and the polymer of the prosthesis by its pro-inflammatory effect, all this resulting in endothelial denudation and risk of very late stent stenosis [19]. As for intra-cardiac devices, the surgical explantation showed incomplete device coverage and presence of thrombus in some cases, sometimes years after implantation [3].

With all of these potential device-related complications, patients should be screened for device compatibility, and high-risk patients should be selected by non-invasive assessment of device coverage. This strategy was well developed for all devices in the in vitro setting and in vivo for intra-vascular devices. Yet, it remains challenging in vivo for intra-cardiac devices.

Objectives

This review aims to (1) present the experimental models used to study this process on cardiac devices; (2) focus on the in vitro techniques and invasive modalities used currently in humans for intra-vascular and intra-cardiac devices and (3) assess the future developments of non-invasive techniques in animal models and humans for intra-cardiac devices.

Experimental models to study the healing process after intra-vascular and intra-cardiac device implantation

Animal models were developed to study the healing process after device implantation, especially after stent positioning. An ideal animal model should reflect the evolution of healing processes in humans, allowing understanding of the genesis of complications, such as stenosis, and guidance for post-implantation treatment [20]. This process appears to be similar in animals and humans in terms of the healing response, but the duration is much longer in humans. However, the selection of the animal is not benign as several factors can interfere with the healing process: species in terms of duration of the healing process; senescence of the animal as a longer duration of healing process exists for older animals; anatomical dimensions and graft surface/vessel caliber that will interfere with blood flow conditions [21, 22]. Cost-effectiveness, accessibility, time frame of the healing process, post-operative risk of death and cellular imaging tools available are other factors that will be useful to decide which model should be retained [20].

Animal models for intra-vascular devices

Intra-vascular devices include stents and vascular prosthesis. Stents have been widely studied starting with bare-metal stents, then followed by drug-eluting stents. Drug-eluting stents allow localized elution of neointimal inhibiting drugs (sirolimus, paclitaxel, everolimus…) and prevent in-stent restenosis. Absorbable drug reservoirs and platforms have been then developed followed by bio-engineered stents coated with antibodies specific to CD 34 to capture circulating endothelial progenitor cells [15].

Intra-vascular device healing processes has been extensively studied.

Animal models are therefore well developed and cross-compared, from small

animals such as rats [20, 23, 24, 25] and rabbits [2, 7, 8, 26, 27, 28, 29, 30] to large animals such as sheep [31, 32, 33], pigs [1, 5, 24, 34, 35, 36, 37, 38, 39, 40], baboons [41] and dogs [25]. Mouse models can serve to assess very small conduit (less than 2 mm) healing processes with serial examinations, small synthetic tubular vascular grafts made of multicellular spheroids [42] or decellularized extracellular matrix [43], and to study the molecular mechanisms of graft failure in pre-clinical assessment [20]. Rabbits are recommended for small vascular grafts (1–4 mm). Studies involving the closest anatomic and physiologic relatives to humans, the primates, are few. But some studies were conducted to assess the healing process after vascular graft and stent implantation, showing 60% of ePTFE artery conduits fully endothelialized after 12 months [44] and demonstrating the reduction of intimal hyperplasia with heparin-coated balloon-expandable stents compared with non-coated stents [45]. However, due to the cost and protected status of primates, alternative large animal models grew momentum. The use of dogs was assessed for vascular graft studies. However, because of a marked difference with the human hemostatic system and a lack of relevance to study graft patency and endothelialization, sheep and pigs were finally preferred [22]. Their availability, low cost, size/anatomy and blood/coagulation systems were found to better complement humans, especially for 4–6 mm grafts. Sheep are closer matches to human results for vascular graft studies and pigs for coronary stents. Sheep present a coagulation system closer to humans than pigs, with few post-operative complications; therefore an appropriate model to assess patency and anastomotic intimal hyperplasia after graft implantation [22]. Pigs are suitable to assess stent patency, calcification and endothelialization albeit with faster healing kinetics than in humans. The influence of ageing and growth on device efficacy and longevity is an important parameter for infantile and adolescent patients. Pigs present an appropriate model with most common strains having indeterminate growth.

Animal models for intra-cardiac devices

Intra-cardiac devices include bioprosthetic heart valves and cardiac defect occluders. Bioprosthetic valves are usually created from animal valve leaflets mounted on a polymer material stent. Atrial septal defect occluders are mostly made of nickel-titanium skeleton and biostable membranes such as PET and e-PTFE membrane. Biodegradable materials are in development. Intra-cardiac

device investigations have been primarily studied in sheep and pig models. The sheep is one of the most widely used animal models for bioprosthetic heart valve and tissue-engineered valve investigations [6, 46, 47, 48]. Such models have enabled pre-clinical evaluations comprising of leaflet motion; effective orifice area; mechanical properties; remodeling of the extracellular matrix; endothelialization and calcification. As for septal defect occluders, experimental models were necessary to assess the healing process [49] and biocompatibility after implantation [4]. Before placing the device, a defect must be created in the fossa ovalis, by transeptal puncture. Pig and sheep models were selected thanks to their close anatomy of the fossa ovalis and dimensions representative of humans, with a special interest in pigs for assessment of device longevity during growth.

AQ2

Bioengineering and in vitro models

Bio-engineered small-diameter vascular grafts consist of a biodegradable scaffold on which endothelial cells are cultured [50]. Customizing the cell populations and neotissue formations in vitro is one of the major goals of this technique. Instead of using a static system to enhance cell culture of the scaffold, a tubular perfusion system bioreactor was developed, allowing a greater maturation and differentiation of cells [51].

The influence of stent struts on local blood flow and the migration of endothelial cells were also studied on in vitro models, using a flow chamber that mimic the geometry of stent struts. It was shown that unidirectional flow leads to a unified forward migration of cells in the flow direction, whereas in the presence of bidirectional flow, complex non-uniform distributions were observed [52].

Human studies

Explanted grafts and devices directly from humans have enabled the study of neotissue formation after implantation. Farb et al. provided a detailed histological study of 116 coronary stents, identifying a spectrum of risk factors for stenosis [13]. A central segment of in vitro femoropopliteal bypass was analyzed 41 months after implantation by Deutsch et al., showing the presence of a mature endothelium covering the graft [14]. Experiments on human homograft valves were also used to investigate the influence of valve-preservation

techniques on endothelial cell growth [53]. Tissue-engineered pulmonary valves could also be studied after explantation from humans, allowing a cross-sectional study of magnetic resonance imaging (MRI) and histology to better understand graft failure mechanisms [54]. Atrial and ventricular septal defect occluders were studied after surgical explantation by Foth et al., providing crucial information about the neotissue formation from five days to four years post-implantation [3].

In vitro techniques to assess the healing process on devices

Histology, the gold standard

Histology is the gold standard to evaluate the healing process, as it allows the most accurate characterization of the tissue covering the device [34]. As the device is metallic, the choice of embedding process before histological and immunohistochemical analysis is important. The hard resin inclusion should be preferred to paraffine inclusion in order to preserve the interface tissue-implant and allow assessment of local processes [3]. Standard histology includes hematoxylin and eosin staining and Richardson blue staining to distinguish cells and scaffold material; Lawson van Gieson, Masson trichrome and Movat pentachrome stainings to detect collagen fibers [35, 54]. Immunohistochemistry has also been applied to characterize specific cell types: von Willebrand factor, CD31 and CD34 for endothelial cells [5, 35, 42]; CD 68 for macrophages, CD 79 for B- and CD 3 for T- cells, CD 45 for leukocytes, CD 34 for endothelial cells progenitors [3, 54, 55]. Inflammation and endothelialization scores involving the extent and severity of inflammation, thrombus/fibrin formation and recellularization of graft tissue can help to better evaluate the healing process [35, 54, 56]. Specific scores concern intimal fibrin content for stent struts [7, 36] and endothelialization extension [36]. Serial examinations on animal and human models have further enabled descriptions of the time frame of the healing process [3, 7, 8] (Fig. 1).

Fig. 1

Histology example. Overview of an Amplatzer atrial septal defect-occlusion device 24 months after implantation. Micrographs show representative staining with Richardson blue (cellular components, blue; metal wires, black). Overview of an Amplatzer atrial septal defect–occlusion device 24 months after implantation. **a** Representative image of pattern of neotissue within the implant with irregular

orientation of cells (detail). **b** Representative image of pattern of cells of pseudointima with longitudinal orientation (parallel to the neoendothelium, detail)

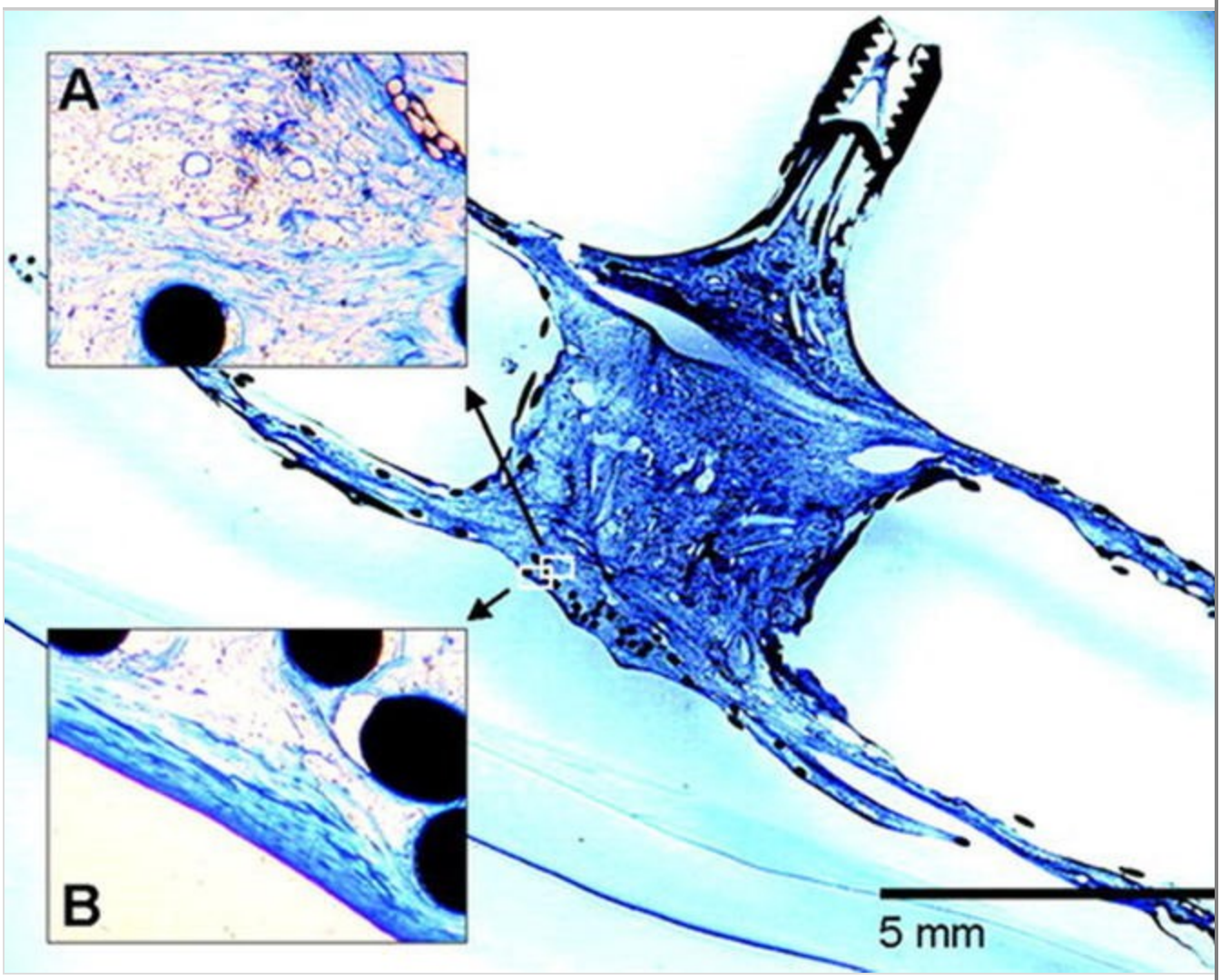

Microscopy techniques

Microscopy techniques are used to characterize the coverage of tissue on cardiac devices. While light microscopy is still important to magnify histologic slides, scanning electron microscopy is largely used in vascular graft engineering [7, 14, 20]. This high-resolution electron-based technique can provide 3D images of the surface covering a stent or a scaffold [7, 20, 31] (Fig. 2). Local organization and the interactions of neotissue with devices can also be investigated [31]. Quantifying endothelialized area [7, 8, 37] and characterizing the time-frame of the healing process [23] can also be performed by studying stent struts coverage by smooth muscle cells, collagen and endothelium after stent implantation.

Moreover, incomplete endothelialized protruding parts of the metal framework after atrial septal defect-occlusion device implantation can be identified [4, 14, 20, 24]. Regions of devices lacking coverage typically show adherence of platelets and macrophages [7].

Fig. 2

Scanning electron microscopy example. Magnified scanning electron microscopy views of overlapping Absorb (Everolimus-eluting bioresorbable vascular scaffold). Magnified scanning electron microscopy (SEM) view of the overlapping Absorb at 28 days (upper), demonstrating multiple uncovered Absorb struts primarily secondary to the direct overlay configuration of the “stacked inner” struts (white asterisks) to the corresponding “stacked outer” struts located abluminally. At 90 days (lower), all “stacked inner” struts (white asterisks) are covered.

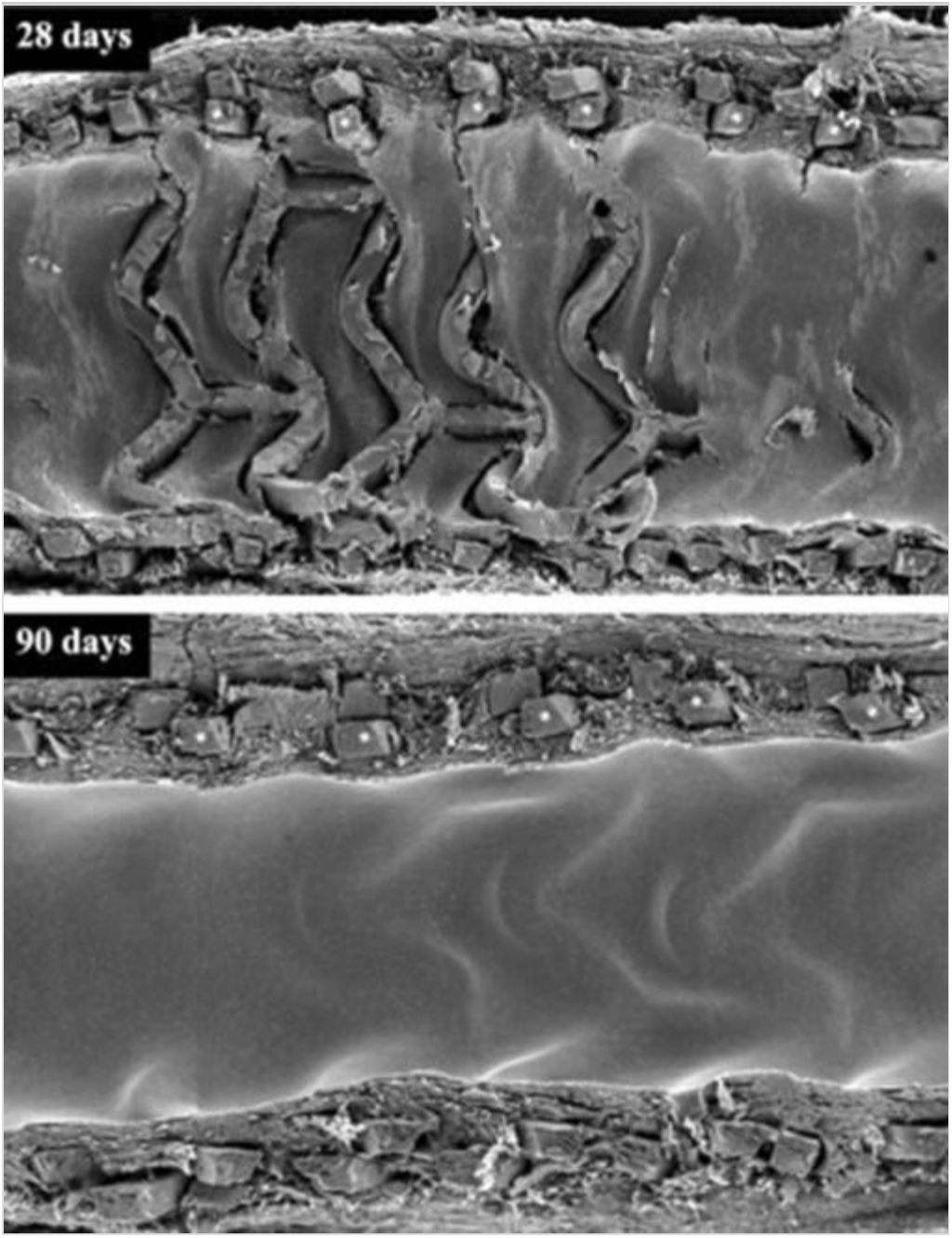

Transmission microscopy is another microscopic technique with a nanometric resolution, higher than scanning electron microscopy. It enables to appreciate the ultrastructure of the components of the neotissue and characterize more precisely the cells [14].

Two-photon microscopy or multi-photon microscopy, is a fluorescent imaging approach that combines a deep penetration and high resolution [1, 50]. Collagen, elastin and endothelial cells can be distinguished, as well as their localization in the tissue [1].

Fiber optic-based imaging

An vitro imaging technique, described by Whited and al [50], consists of mapping fluorescently labelled endothelial cells placed in a half-vessel scaffold. A micro-imaging channel is embedded in the wall of a scaffold through which the excitation fiber optic is inserted. The endothelial cell fluorescence may then be captured by a photosensitive detector to map the cell distributions within the scaffold. This allows for non-destructive, dynamic imaging of the endothelium of the vascular graft with no impact on the adjacent structures.

Invasive techniques available in humans

Histology and microscopy techniques can only be used on explanted devices. Intra-vascular ultrasounds (IVUS) and optical coherence tomography (OCT) were developed for intra-vascular grafts, allowing an invasive evaluation of the healing process on stents.

Intra-vascular ultrasounds

This invasive, catheter-based technique relies on the use of ultrasound impulses, emitted from a miniaturized transducer, mounted on the tip of a catheter [57]. It provides real-time, cross-sectional tomographic images of the internal surface of the blood vessel [58, 59]. The axial resolution is around 50 μm, depending on the catheter type. High ultrasound reflection between variable tissue interfaces enables differentiation of the layers of the vessel wall [57].

It can be used to evaluate a vessel in terms of lesion quantification and morphology assessment: before or after stent implantation or vascular grafting with higher sensitivity in assessing coronary artery lumen morphology [60] (Fig. 3), after cardiac transplantation to detect coronary transplant vasculopathy and for evaluation of atherosclerotic plaque formation [7, 57, 58].

Fig. 3

OCT and IVUS example. OCT evidence of uncovered struts in drug-eluting stent late stent thrombosis. Representative angiographic (**a**), intravascular ultrasound (**b**–**d**), and optical coherence tomography (**e**–**g**) cross-sectional images from a patient with very late stent thrombosis at 1836 days in a single sirolimus-eluting stent implanted in proximal left anterior descending artery. After thrombus aspiration, uncovered struts are detected by OCT, with remaining intraluminal thrombus

adherent to some strut. Positive remodeling was not observed by IVUS.

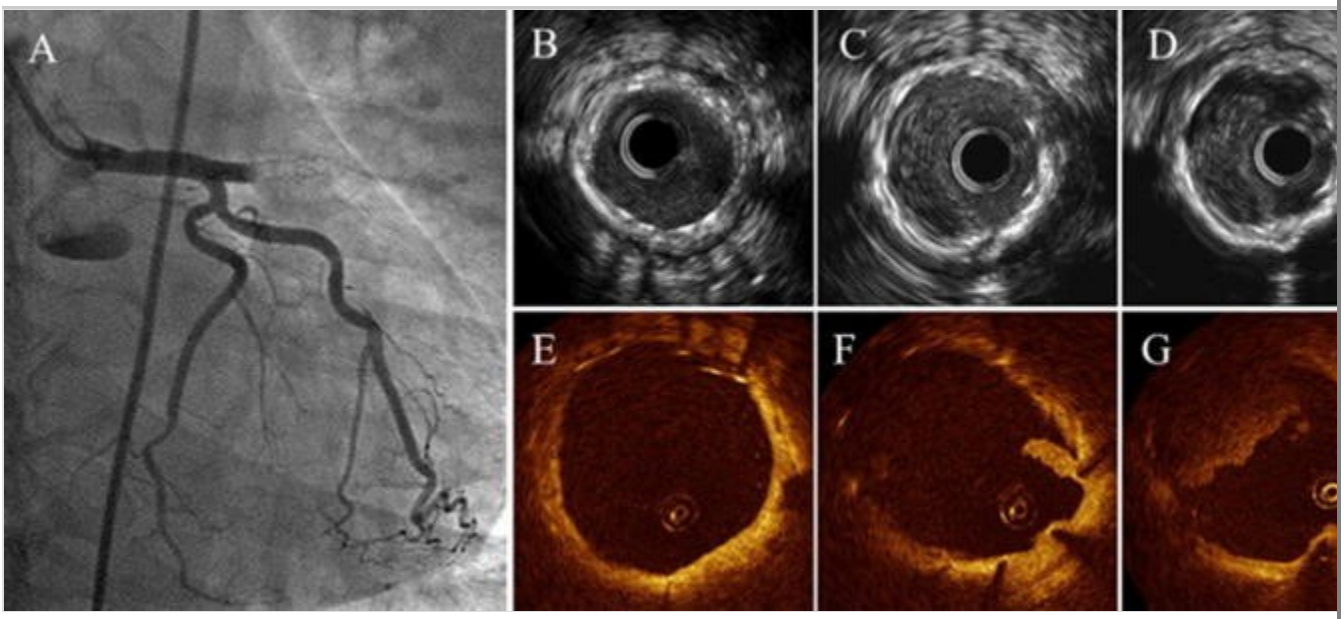

To customize the technique, the near-infrared spectroscopy imaging system was incorporated in the IVUS catheter and used to analyze the atherosclerotic plaque composition [57]. The reflected signal is converted in a chemogram that represents a color map of the location of lipid core plaques to characterize the composition of the plaque and select patients at high-risk of adverse outcome [57].

IVUS has not been extended to other devices, especially intra-cardiac devices such as occluders.

Intravascular optical coherence tomography

OCT is a near-infrared light-based modality that provides high resolution imaging (10 μm for axial resolution and 20–40 μm for lateral resolution) of the microstructure of the tissue and blood vessel wall in vivo [26, 34, 61].

In the interventional cardiology field, this invasive technique is used to evaluate the microstructure of the vessels, atheroma plaque and stents [34, 62] (Fig. 3). The OCT catheter is placed at the distal part of the stent and the entire length of the region is scanned using the integrated automated pullback device [26, 34, 57].

OCT enables distinction of the three layers of the vessels, to identify lesions such as unstable atherosclerotic plaques, macrophage accumulations and thrombi [61]. For stented arteries, neointimal hyperplasia can be detected [63, 64] and a morphometric analysis of the stent strut coverage can be performed [63, 65]. Dissection of stents, noncoverage, calcification and misalignment of struts may also be detected [17, 26, 34, 57, 61, 66]. Such information can thus far only be obtained in vivo using OCT, thanks to its 10-fold higher resolution than IVUS [67], which has successfully been applied to guide pharmalogical therapy for the prevention of late stent thrombosis [26]. It is also used in tissue-bioengineering, but to date, has not been evaluated in the assessment of intra-cardiac device coverage [68]. One of the drawbacks of this technique is the inability to detect the endothelial layers that measure less than 10 μm and complications due to the invasiveness of the procedure [68].

Future developments of non-invasive techniques in animal models and humans

MRI

In cardiovascular tissue engineering, MRI is used as a non-invasive technique to monitor the remodeling of vascular grafts and their patency, to follow the cells implanted in vitro in the graft and to evaluate inflammation and thrombosis after implantation [31, 69]. This is made possible by the adjunction of ultra-small superparamagnetic iron oxide biocompatible particles in the scaffold to render it visible and provide morphological information of the graft [31, 69].

In humans, even if most of the modalities have been developed for intra-vascular devices, imaging the tissue covering intra-cardiac devices, such as septal occluders or left atrial appendage occlusion devices, is also challenging and clinically relevant.

Thanks to its high spatial and temporal resolutions, significant focus has been applied to tissue characterization using MRI [70, 71, 72], especially to detect myocardial fibrosis [73], myocardial edema and microvascular obstruction [70]. Fibrosis can be identified by late gadolinium enhancement, favored for visualization of myocardial focal fibrotic scar [74], as seen in ischemic and non-ischemic cardiomyopathy. T1 and T2 MRI provides has further been used to enhance images of fibrotic, inflammatory and edematous tissue [75, 76, 77].

Intra-cardiac imaging devices, has been mostly used to detect device position and cardiac remodeling after implantation [78]. Yet, work is still to be done to optimize MRI for neo-tissue detection due to challenges associated with the required resolution and to alleviate image artefacts, particularly due to the metal framework of the prosthesis, especially occlude screw hubs.

Computed tomography

Computed tomography [CT] is known to detect focal myocardial fibrotic scars [74], providing an infra-millimetric resolution (0.5 mm compared to 1–2 mm for MRI) [79, 80].

Multidetector computed tomography angiography and ultra-high-resolution computed tomography angiography are now in development to detect coronary stent stenosis. Thanks to its higher temporal and spatial resolution than 4 and 16-slice CT, 64-slice multidetector computed tomography angiography presents a good correlation with angiography and IVUS for detection of diameter and area stent stenosis for > 3 mm stents. The motion and blooming artefacts are less important but the temporal resolution is not as good as IVUS [81]. For calcified lesions, ultra-high-resolution CT presents fewer artefacts and a better spatial resolution for in-stent lumen assessment > 2.5 mm [82].

Regarding intra-cardiac devices, cardiac CT is mostly used for the follow-up of patients after percutaneous left atrial appendage occlusion to assess the presence of device thrombosis and peri-device leaks and to guide post-procedural anti-thrombotic therapy durations [83, 84]. However, for some cases, cardiac CT cannot discriminate between laminated thrombus (reinforcement of anti-thrombotic treatment recommended) and locally prominent device covering (no treatment needed).

Thus, dedicated CT sequences to precisely identify the fibrotic tissue covering intra-cardiac devices could provide improved tailored patient management.

Sensors to detect endothelialization on coronary stents

Musick and al. [18]. described the use of a piezoelectric microcantilever placed in the strut of an active stent to detect endothelialization of the struts. When cells attach to the cantilever, they cause an increase in mass and decrease in the resonant frequencies of the cantilever. The goal of this non-invasive process is to

monitor the healing process after stent implantation, but without the possibility to differentiate the types of covering tissues (endothelium versus fibrin). There is potential future clinical application of such sensors to provide non-invasive follow-up of healing status and determine the patient's anti-platelet therapy. An approach beneficial to intra-vascular devices but also intra-cardiac applications.

High frame rate ultrasound imaging

Noninvasive high frame rate ultrasound imaging may be a promising technique to detect neotissue formation. It was recently experienced in different fields of cardiology, notably to visualize the epicardial and intramural coronary vasculature to assess coronary microcirculation and coronary blood flow in normal and pathologic situations. It offers a visualization of the pre-arteriolar coronary vessel structure which size is 100 to 500 microns, in animals and humans [85]. The shear wave imaging that relies on the mapping of the propagation velocities of shear waves related to tissue viscoelastic properties is another technique in development [86, 87].

Conclusion

Imaging neotissue covering a cardiac device is a necessary step yet remains challenging. In vitro techniques, such as histology, remain the gold standard even if several invasive techniques (OCT, IVUS) have been developed to detect vessel structure and coronary stent restenosis. Most of these techniques were developed for intra-vascular devices. With the evolution of MRI and CT imaging of cardiac fibrosis, we hope that such techniques will provide insight in to neotissue intra-cardiac device coverage in the near future.

AQ3

Publisher's Note

Acknowledgements

The figures were reprinted: Fig. 1: reprinted from Circulation: Cardiovascular Interventions 2009;2:90–96, by Foth et al., Immunohistochemical characterization of neotissues and tissue reactions to septal defect-occlusion

devices, Figure n°1, Copyright 2009, with permission from Wolters Kluwer Health, Inc. Fig. 2: reprinted from JACC: Cardiovascular Interventions 2013;6[5]:523−32, by Farooq et al., Intracoronary optical coherence tomography and histology of overlapping everolimus-eluting bioresorbable vascular scaffolds in a porcine coronary artery model the potential implications for clinical practice, Figure n°7, Copyright 2013, with permission from Elsevier Inc. Fig. 3: reprinted from JACC: Cardiovascular Interventions 2012;5[1]:12–20, by Guagliumi et al., Examination of the in vivo mechanisms of late drug-eluting stent thrombosis-Findings from optical coherence tomography and intravascular ultrasound imaging, Figure n°1, Copyright 2012, with permission from Elsevier Inc.

Funding

This study received financial support from the French Government as part of the "Investments of the Future" program managed by the National Research Agency (ANR), Grant reference ANR-10-IAHU-04.

Compliance with Ethical Standards

Ethical approval The manuscript does not contain clinical studies or patient data.

References

1. Dahan N, Sarig U, Bronshtein T, Baruch L, Karram T, Hoffman A et al (2017) Dynamic autologous reendothelialization of small-caliber arterial extracellular matrix: a preclinical large animal study. Tissue Eng Part A 23:69–79. https://doi.org/10.1089/ten.tea.2016.0126

2. Liu J, Peng Y, Lai J, Gao W, Song A, Zhang G (2017) Fluid upstream shear stress of rabbit aortic stenosis inhibits neointimal hyperplasia by promoting endothelization after balloon injury. BMC Cardiovasc Disord 17:273. https://doi.org/10.1186/s12872-017-0690-3

3. Foth R, Quentin T, Michel-Behnke I, Vogt M, Kriebel T, Kreischer A et al (2009) Immunohistochemical characterization of neotissues and tissue reactions to septal defect-occlusion devices. Circ Cardiovasc Interv 2:90–96. https://doi.org/10.1161/circinterventions.108.810507

4. Sigler M, Jux C (2007) Biocompatibility of septal defect closure devices. Heart 93:444–449. https://doi.org/10.1136/hrt.2006.098103

5. Pislaru SV, Harbuzariu A, Agarwal G, Witt T, Gulati R, Sandhu NP et al (2006) Magnetic forces enable rapid endothelialization of synthetic vascular grafts. Circulation 114:314–318. https://doi.org/10.1161/circulationaha.105.001446

6. Syedain Z, Reimer J, Schmidt J, Lahti M, Berry J, Bianco R et al (2015) 6-month aortic valve implantation of an off-the-shelf tissue-engineered valve in sheep. Biomaterials 73:175–184. https://doi.org/10.1016/j.biomaterials.2015.09.016

7. Cheneau E, John MC, Fournadjiev J, Chan RC, Kim HS, Leborgne L et al (2003) Time course of stent endothelialization after intravascular radiation therapy in rabbit iliac arteries. Circulation 107:2153–2158. https://doi.org/10.1161/01.CIR.0000062648.39025.09

8. Finn AV, Kolodgie FD, Harnek J, Guerrero LJ, Acampado E, Tefera K (2005) Differential response of delayed healing and persistent inflammation at sites of overlapping sirolimus- or paclitaxel-eluting stents. Circulation 112:270–278. https://doi.org/10.1161/circulationaha.104.508937

9. Virmani R, Kolodgie FD, Farb A, Lafont A (2003) Drug eluting stents: are human and animal studies comparable? Heart Br Card Soc 89:133–138

10. Takano M, Yamamoto M, Inami S, Murakami D, Seimiya K, Ohba T et al (2008) Long-term follow-up evaluation after sirolimus-eluting stent implantation by optical coherence tomography. J Am Coll Cardiol 51:968–969

11. Chen F, Zhao X, Zheng X, Chen S, Xu R, Qin Y (2011) Incomplete endothelialization and late dislocation after implantation of an Amplatzer septal occluder device. Circulation 124:188–189. https://doi.org/10.1161/circulationaha.110.991836

12. Nguyen AK, Palafox BA, Starr JP, Gates RN, Berdjis F (2016)

Endocarditis and incomplete endothelialization 12 years after Amplatzer septal occluder deployment. Tex Heart Inst J 43:227–231. https://doi.org/10.14503/THIJ-14-4949

13. Farb A, Weber DK, Kolodgie FD, Burke AP, Virmani R (2002) Morphological predictors of restenosis after coronary stenting in humans. Circulation 105:2974–2980. https://doi.org/10.1161/01.CIR.0000019071.72887.BD

14. Deutsch M, Meinhart J, Vesely M, Fischlein T, Groscurth P, von Oppell U et al (1997) In vitro endothelialization of expanded polytetrafluoroethylene grafts: a clinical case report after 41 months of implantation. J Vasc Surg 25:757–763

15. Pendyala LK, Yin X, Li J, Chen JP, Chronos N, Hou D (2009) The first-generation drug-eluting stents and coronary endothelial dysfunction. JACC Cardiovasc Interv 2:1169–1177. https://doi.org/10.1016/j.jcin.2009.10.004

16. Li S, Gai L, Yang T, Zhang L, Xu X, Bai Q et al (2013) Evaluation of long-term follow-up with neointimal coverage and stent apposition after sirolimus-eluting stent implantation by optical coherence tomography. Catheter Cardiovasc Interv 81:768–775. https://doi.org/10.1002/ccd.24497

17. Gonzalo N, Barlis P, Serruys PW, Garcia-Garcia HM, Onuma Y, Ligthart J et al (2009) Incomplete stent apposition and delayed tissue coverage are more frequent in drug-eluting stents implanted during primary percutaneous coronary intervention for ST-segment elevation myocardial infarction than in drug-eluting stents implanted for stable/unstable angina. JACC Cardiovasc Interv 2:445–452. https://doi.org/10.1016/j.jcin.2009.01.012

18. Musick KM, Coffey AC, Irazoqui PP (2010) Sensor to detect endothelialization on an active coronary stent. Biomed Eng OnLine 9:67. https://doi.org/10.1186/1475-925X-9-67

19. Foin N, Gutierrez-Chico JL, Nakatani S, Torii R, Bourantas CV, Sen S et al (2014) Incomplete stent apposition causes high shear flow disturbances and delay in neointimal coverage as a function of strut to wall detachment

distance: implications for the management of incomplete stent apposition. Circ Cardiovasc Interv 7:180–189. https://doi.org/10.1161/circinterventions.113.000931

20. Chan AH, Tan RP, Michael PL, Lee BS, Vanags LZ, Ng MKC et al (2017) Evaluation of synthetic vascular grafts in a mouse carotid grafting model. PLOS ONE 12:e0174773. https://doi.org/10.1371/journal.pone.0174773

21. Zilla P, Bezuidenhout D, Human P (2007) Prosthetic vascular grafts: wrong models, wrong questions and no healing. Biomaterials 28:5009–5027. https://doi.org/10.1016/j.biomaterials.2007.07.017

22. Byrom MJ, Bannon PG, White GH, Ng MKC (2010) Animal models for the assessment of novel vascular conduits. J Vasc Surg 52:176–195. https://doi.org/10.1016/j.jvs.2009.10.080

23. Mirza A, Hyvelin JM, Rochefort GY, Lermusiaux P, Antier D, Awede B et al (2008) Undifferentiated mesenchymal stem cells seeded on a vascular prosthesis contribute to the restoration of a physiologic vascular wall. J Vasc Surg 47:1313–1321. https://doi.org/10.1016/j.jvs.2007.12.038

24. Wang TJ, Yang YJ, Xu B, Zhang Q, Jin C, Tang Y et al (2012) Atorvastatin accelerates both neointimal coverage and re-endothelialization after sirolimus-eluting stent implantation in a porcine model. Circ J 76:2561–2571. https://doi.org/10.1253/circj.CJ-12-0468

25. Liu HT, Li F, Wang WY, Li XJ, Liu YM, Wang RA et al (2010) Rapamycin inhibits re-endothelialization after percutaneous coronary intervention by impeding the proliferation and migration of endothelial cells and inducing apoptosis of endothelial progenitor cells. Tex Heart Inst J 37:194–201

26. Prati F, Romagnoli E, Valgimigli M, Burzotta F, De Benedictis M, Ramondo A et al (2014) Randomized comparison between 3-month Cre8 DES vs. 1-month Vision/Multilink8 BMS neointimal coverage assessed by OCT evaluation: The DEMONSTRATE study. Int J Cardiol 176:904–909.

https://doi.org/10.1016/j.ijcard.2014.08.031

27. Ma X, Hibbert B, Dhaliwal B, Seibert T, Chen YX, Zhao X et al (2010) Delayed re-endothelialization with rapamycin-coated stents is rescued by the addition of a glycogen synthase kinase-3β inhibitor. Cardiovasc Res 86:338–345. https://doi.org/10.1093/cvr/cvq047

28. Tang C, Wang G, Wu X, Li Z, Shen Y, Lee JC et al (2011) The impact of vascular endothelial growth factor-transfected human endothelial cells on endothelialization and restenosis of stainless steel stents. J Vasc Surg 53:461–471. https://doi.org/10.1016/j.jvs.2010.08.020

29. Toma C, Fisher A, Wang J, Chen X, Grata M, Leeman J et al (2011) Vascular endoluminal delivery of mesenchymal stem cells using acoustic radiation force. Tissue Eng Part A 17:1457–1464. https://doi.org/10.1089/ten.tea.2010.0539

30. Larsen K, Cheng C, Tempel D, Parker S, Yazdani S, den Dekker WK et al (2012) Capture of circulatory endothelial progenitor cells and accelerated re-endothelialization of a bio-engineered stent in human ex vivo shunt and rabbit denudation model. Eur Heart J 33:120–128. https://doi.org/10.1093/eurheartj/ehr196

31. Mertens ME, Koch S, Schuster P, Wehner J, Wu Z, Gremse F et al (2015) USPIO-labeled textile materials for non-invasive MR imaging of tissue-engineered vascular grafts. Biomaterials 39:155–163. https://doi.org/10.1016/j.biomaterials.2014.10.076

32. Koobatian MT, Row S, Smith RJ Jr, Koenigsknecht C, Andreadis ST, Swartz DD (2016) Successful endothelialization and remodeling of a cell-free small-diameter arterial graft in a large animal model. Biomaterials 76:344–358. https://doi.org/10.1016/j.biomaterials.2015.10.020

33. Fukunishi T, Best CA, Sugiura T, Shoji T, Yi T, Udelsman B et al (2016) Tissue-engineered small diameter arterial vascular grafts from cell-free nanofiber PCL/Chitosan scaffolds in a sheep model. PLOS ONE 11(7):158555. https://doi.org/10.1371/journal.pone.0158555.

34. Attizzani G, Bezerra H, Chamié D, Fujino Y, Spognardi A, Stanley J et al (2012) Serial evaluation of vascular response after implantation of a new sirolimus-eluting stent with bioabsorbable polymer [MISTENT]: an optical coherence tomography and histopathological study. J Invasive Cardiol 24(11):560–568

35. Ruiter MS, Doornbos A, de Waard V, de Winter RJ, Attevelt NJM, Steendam R et al (2016) Long-term effect of stents eluting 6-mercaptopurine in porcine coronary arteries. J Negat Results Biomed 15:15–20. https://doi.org/10.1186/s12952-016-0063-y

36. Wittchow E, Adden N, Riedmüller J, Savard C, Waksman R, Braune M (2013) Bioresorbable drug-eluting magnesium-alloy scaffold: design and feasibility in a porcine coronary model. EuroIntervention 8:1441–1450. https://doi.org/10.4244/EIJV8I12A218

37. Zhang B, Zheng B, Wang X, Shi Q, Jia J, Huo Y et al (2017) Polymer-free dual drug-eluting stents evaluated in a porcine model. BMC Cardiovasc Disord 17:222. https://doi.org/10.1186/s12872-017-0654-7

38. Koppara T, Joner M, Bayer G, Steigerwald K, Diener T, Wittchow E (2012) Histopathological comparison of biodegradable polymer and permanent polymer based sirolimus eluting stents in a porcine model of coronary stent implantation. Thromb Haemost 107:1161–1171. https://doi.org/10.1160/TH12-01-0043

39. Rotmans JI, Heyligers JM, Verhagen HJ, Velema E, Nagtegaal MM, Kleijn DP et al (2005) In vivo cell seeding with anti-CD34 antibodies successfully accelerates endothelialization but stimulates intimal hyperplasia in porcine arteriovenous expanded polytetrafluoroethylene grafts. Circulation 112:12–18. https://doi.org/10.1161/circulationaha.104.504407

40. Farooq V, Serruys PW, Heo JH, Gogas BD, Onuma Y, Perkins LE et al (2013) Intracoronary optical coherence tomography and histology of overlapping everolimus-eluting bioresorbable vascular scaffolds in a porcine coronary artery model. JACC Cardiovasc Interv 6:523–532. https://doi.org/10.1016/j.jcin.2012.12.131

41. Jordan SW, Haller CA, Sallach RE, Apkarian RP, Hanson SR, Chaikof EL (2007) The effect of a recombinant elastin-mimetic coating of an ePTFE prosthesis on acute thrombogenicity in a baboon arteriovenous shunt. Biomaterials 28:1191–1197. https://doi.org/10.1016/j.biomaterials.2006.09.048

42. Itoh M, Nakayama K, Noguchi R, Kamohara K, Furukawa K, Uchihashi K et al (2015) Scaffold-free tubular tissues created by a Bio-3D printer undergo remodeling and endothelialization when implanted in rat aortae. PLOS ONE 10:e0136681. https://doi.org/10.1371/journal.pone.0136681

43. Aubin H, Mas-Moruno C, Iijima M, Schütterle N, Steinbrink M, Assmann A et al. Customized interface biofunctionalization of decellularized extracellular matrix: toward enhanced endothelialization. Tissue Eng Part C Methods 22 (2016) 496–508. https://doi.org/10.1089/ten.tec.2015.0556

44. Clowes AW, Gown AM, Hanson SR, Reidy MA (1985) Mechanisms of arterial graft failure. Role of cellular proliferation in early healing of PTFE prostheses. Am J Pathol 118:43–54

45. Lin PH, Chronos NA, Marijianowski MM, Chen C, Conklin B, Bush RL et al. Carotid stenting using heparin-coated balloon-expandable stent reduces intimal hyperplasia in a baboon model. J Surg Res 112 (2003) 84–90. https://doi.org/10.1016/S0022-4804(03)00124-0

46. Vincentelli A, Wautot F, Juthier F, Fouquet O, Corseaux D, Marechaux S et al. In vivo autologous recellularization of a tissue-engineered heart valve: Are bone marrow mesenchymal stem cells the best candidates? J Thorac Cardiovasc Surg 134 (2007) 424–432. https://doi.org/10.1016/j.jtcvs.2007.05.005

47. Schmitt B, Spriestersbach H, h-Ití DO, Radtke T, Bartosch M, Peters H et al (2016) Percutaneous pulmonary valve replacement using completely tissue-engineered off-the-shelf heart valves: six-month in vivo functionality and matrix remodelling in sheep. EuroIntervention 12:62–70. https://doi.org/10.4244/EIJV12I1A12

48. Hof A, Raschke S, Baier K, Nehrenheim L, Selig JI, Schomaker M et al. Challenges in developing a reseeded, tissue-engineered aortic valve prosthesis. Eur J Cardiothorac Surg 50 (2016) 446–455. https://doi.org/10.1093/ejcts/ezw057

49. Milewski K, Fiszer R, Buszman PP, Węglarz P, Janas A, Krauze A et al (2017) Temporal healing patterns and coverage dynamics after new polish transcatheter PFO occluder implantation in a swine. Kardiol Pol 75:907–913. https://doi.org/10.5603/KP.a2017.0117

50. Whited BM, Hofmann MC, Lu P, Xu Y, Rylander CG, Wang G et al. Dynamic, nondestructive imaging of a bioengineered vascular graft endothelium. PLoS ONE 8 (2013) e61275. https://doi.org/10.1371/journal.pone.0061275

51. Melchiorri AJ, Bracaglia LG, Kimerer LK, Hibino N, Fisher JP. In vitro endothelialization of biodegradable vascular grafts via endothelial progenitor cell seeding and maturation in a tubular perfusion system bioreactor. Tissue Eng Part C Methods 22 (2016) 663–670. https://doi.org/10.1089/ten.tec.2015.0562

52. Hsiao ST, Spencer T, Boldock L, Prosseda SD, Xanthis I, Tovar-Lopez FJ et al. Endothelial repair in stented arteries is accelerated by inhibition of Rho-associated protein kinase. Cardiovasc Res 112 (2016) 689–701. https://doi.org/10.1093/cvr/cvw210

53. Eberl T, Siedler S, Schumacher B, Zilla P, Schlaudraff K (1992) R. Fasol. Experimental in vitro endothelialization of cardiac valve leaflets. Ann Thorac Surg 53:487–492

54. Voges I, Bräsen JH, Entenmann A, Scheid M, Scheewe J, Fischer G et al. Adverse results of a decellularized tissue-engineered pulmonary valve in humans assessed with magnetic resonance imaging. Eur J Cardiothorac Surg 44 (2013) 272–279. https://doi.org/10.1093/ejcts/ezt328

55. Aoki J, Serruys PW, van Beusekom H, Ong ATL, McFadden EP, Sianos G et al. Endothelial progenitor cell capture by stents coated with antibody

against CD34. J Am Coll Cardiol 45 (2005) 1574–1579. https://doi.org/10.1016/j.jacc.2005.01.048

56. Kar S, Hou D, Jones R, Werner D, Swanson L, Tischler B et al. Impact of Watchman and Amplatzer devices on left atrial appendage adjacent structures and healing response in a canine model. JACC Cardiovasc Interv 7 (2014) 801–809. https://doi.org/10.1016/j.jcin.2014.03.003

57. Hoang V, Grounds J, Pham D, Virani S, Hamzeh I, Qureshi AM et al. The role of intracoronary plaque imaging with intravascular ultrasound, optical coherence tomography, and near-infrared spectroscopy in patients with coronary artery disease. Curr Atheroscler Rep 18 18 (2016) 57. https://doi.org/10.1007/s11883-016-0607-0

58. Vasquez A, Mistry N, Singh J. Impact of Intravascular Ultrasound in Clinical Practice. Interv Cardiol Rev.9 (2014) 156. https://doi.org/10.15420/icr.2014.9.3.156

59. Erglis A, Narbute I (2014) Intravascular Ultrasound-based Imaging Modalities for Tissue Characterisation. Interv Cardiol Rev 9:151. https://doi.org/10.15420/icr.2014.9.3.151

60. Schiele F, Meneveau N, Vuillemenot A, Zhang DD, Gupta S, Mercier M et al (1998) Impact of intravascular ultrasound guidance in stent deployment on 6-month restenosis rate: a multicenter, randomized study comparing two strategies—with and without intravascular ultrasound guidance. J Am Coll Cardiol 32:320–328

61. Tearney GJ, Regar E, Akasaka T, Adriaenssens T, Barlis P, Bezerra HG et al. Consensus standards for acquisition, measurement, and reporting of intravascular optical coherence tomography studies. J Am Coll Cardiol 59 (2012) 1058–1072. https://doi.org/10.1016/j.jacc.2011.09.079

62. Barlis P, Regar E, Serruys PW, Dimopoulos K, van der Giessen WJ, van Geuns RJ et al. An optical coherence tomography study of a biodegradable vs. durable polymer-coated limus-eluting stent: a LEADERS trial sub-study. Eur Heart J 31 (2010) 165–176. https://doi.org/10.1093/eurheartj/ehp480

63. Murase S, Suzuki Y, Yamaguchi T, Matsuda O, Murata A, Ito T. The relationship between re-endothelialization and endothelial function after DES implantation: Comparison between paclitaxcel eluting stent and zotarolims eluting stent. Catheter Cardiovasc Interv 83 (2014) 412–417. https://doi.org/10.1002/ccd.25140

64. Lehtinen T, Kiviniemi TO, Ylitalo A, Mikkelsson J, Airaksinen JKE, Karjalainen PP (2012) Early vascular healing after endothelial progenitor cell capturing stent implantation. J Invasive Cardiol 24:631–635

65. Bonnema GT, Cardinal KO, Williams SK, Barton JK (2008) An automatic algorithm for detecting stent endothelialization from volumetric optical coherence tomography datasets. Phys Med Biol 53:3083–3098. https://doi.org/10.1088/0031-9155/53/12/001

66. Kobayashi Y, Okura H, Kume T, Yamada R, Kobayashi Y, Fukuhara K et al (2014) Impact of target lesion coronary calcification on stent expansion. Circ J 78:2209–2214

67. Guagliumi G, Sirbu V, Musumeci G, Gerber R, Biondi-Zoccai G, Ikejima H et al (2012) Examination of the in vivo mechanisms of late drug-eluting stent thrombosis. JACC Cardiovasc Interv 5:12–20. https://doi.org/10.1016/j.jcin.2011.09.018

68. Gurjarpadhye AA, DeWitt MR, Xu Y, Wang G, Rylander MN, Rylander CG (2015) Dynamic assessment of the endothelialization of tissue-engineered blood vessels using an optical coherence tomography catheter-based fluorescence imaging system. Tissue Eng Part C Methods 21:758–766. https://doi.org/10.1089/ten.tec.2014.0345

69. Fayol D, Le Visage C, Ino J, Gazeau F, Letourneur D, Wilhelm C (2013) Design of biomimetic vascular grafts with magnetic endothelial patterning. Cell Transplant 22:2105–2118. https://doi.org/10.3727/096368912X661300

70. Bucciarelli-Ducci C, Baritussio A, Auricchio A. Cardiac MRI anatomy and function as a substrate for arrhythmias. EP Eur 18 (2016) 130–135. https://doi.org/10.1093/europace/euw357

71. Haaf P, Garg P, Messroghli DR, Broadbent DA, Greenwood JP, Plein S. Cardiac T1 mapping and extracellular volume in clinical practice: a comprehensive review. J Cardiovasc Magn Reson 18 (2017) 89. https://doi.org/10.1186/s12968-016-0308-4

72. Captur G, Manisty C, Moon JC. Cardiac MRI evaluation of myocardial disease. Heart 102 (2016) 1429–1435. https://doi.org/10.1136/heartjnl-2015-309077

73. Gyöngyösi M, Winkler J, Ramos I, Do QT, Firat H, McDonald K et al. Myocardial fibrosis: biomedical research from bench to bedside: myocardial fibrosis: biomedical research from bench to bedside. Eur J Heart Fail 19 (2017) 177–191. https://doi.org/10.1002/ejhf.696

74. Berliner JI, Kino A, Carr JC, Bonow RO, Choudhury L. Cardiac computed tomographic imaging to evaluate myocardial scarring/fibrosis in patients with hypertrophic cardiomyopathy: a comparison with cardiac magnetic resonance imaging. Int J Cardiovasc Imaging 29 (2013) 191–197. https://doi.org/10.1007/s10554-012-0048-y

75. Ghosn MG, Shah DJ. Important advances in technology and unique applications related to cardiac magnetic resonance imaging. Methodist DeBakey Cardiovasc J 10 (2014) 159–162. https://doi.org/10.14797/mdcj-10-3-159

76. Graham-Brown MPM, Patel AS, Stensel DJ, March DS, Marsh AM, McAdam J et al (2017) Imaging of myocardial fibrosis in patients with end-stage renal disease: current limitations and future possibilities. BioMed Res Int. https://doi.org/10.1155/2017/5453606

77. Puntmann VO, Peker E, Chandrashekhar Y, Nagel E. T1 Mapping in characterizing myocardial disease: a comprehensive review. Circ Res 119 (2016) 277–299. https://doi.org/10.1161/circresaha.116.307974

78. Lapierre C, Hugues N, Dahdah N, Déry J, Raboisson MJ, Miró J. Long-term follow-up of large atrial septal occluder (Amplatzer device) with cardiac MRI in a pediatric population. Am J Roentgenol 199 (2012) 1136–1141.

https://doi.org/10.2214/AJR.12.8617

79. Maron BJ, Maron MS (2016) The remarkable 50 years of imaging in HCM and how it has changed diagnosis and management. JACC Cardiovasc Imaging 9:858–872. https://doi.org/10.1016/j.jcmg.2016.05.003

80. Mahida S, Sacher F, Dubois R, Sermesant M, Bogun F, Haissaguerre M et al. Cardiac imaging in patients with ventricular tachycardia. Circulation 136 (2017) 2491–2507. https://doi.org/10.1161/circulationaha.117.029349

81. Kwon W, Choi J, Kim JY, Kim SY, Yoon J, Choe KH et al (2012) In-stent area stenosis on 64-slice multi-detector computed tomography coronary angiography: optimal cutoff value for minimum lumen cross-sectional area of coronary stents compared with intravascular ultrasound. Int J Cardiovasc Imaging 28:21–31. https://doi.org/10.1007/s10554-012-0057-x

82. Motoyama S, Ito H, Sarai M, Nagahara Y, Miyajima K, Matsumoto R et al. Ultra-high-resolution computed tomography angiography for assessment of coronary artery stenosis. Circ J 82 (2018) 1844–1851. https://doi.org/10.1253/circj.CJ-17-1281

83. Cochet H, Iriart X, Sridi S, Camaioni C, Corneloup O, Montaudon M et al (2018) Left atrial appendage patency and device-related thrombus after percutaneous left atrial appendage occlusion: a computed tomography study. Eur Heart J - Cardiovasc Imaging 19:1351–1361. https://doi.org/10.1093/ehjci/jey010.

84. Marini D, Ou P, Boudjemline Y, Kenny D, Bonnet D, Agnoletti G (2012) Midterm results of percutaneous closure of very large atrial septal defects in children: role of multislice computed tomography. EuroIntervention 7:1428–1434. https://doi.org/10.4244/EIJV7I12A223

85. Maresca D, Correia M, Villemain O, Bizé A, Sambin L, Tanter M et al (2018) Noninvasive imaging of the coronary vasculature using ultrafast ultrasound. JACC Cardiovasc Imaging 11:798–808. https://doi.org/10.1016/j.jcmg.2017.05.021

86. Strachinaru M, Bosch JG, van Dalen BM, van Gils L, van der Steen AFW, de Jong N et al (2017) Cardiac shear wave elastography using a clinical ultrasound system. Ultrasound Med Biol 43:1596–1606. https://doi.org/10.1016/j.ultrasmedbio.2017.04.012

87. Brekke B, Nilsen LCL, Lund J, Torp H, Bjastad T, Amundsen BH et al (2014) Ultra-high frame rate tissue Doppler imaging. Ultrasound Med Biol 40:222–231. https://doi.org/10.1016/j.ultrasmedbio.2013.09.012